THE AMERICAN SOCIETY OF MECHANICAL ENGINEERS
345 E. 47 St., New York, N.Y. 10017

89-GT-276

Surface Injection Effect on Mass Transfer from a Cylinder in Crossflow: A Simulation of Film Cooling in the Leading Edge Region of a Turbine Blade

J. KARNI* and R. J. GOLDSTEIN
Department of Mechanical Engineering
University of Minnesota
Minneapolis, Minnesota 55455

ABSTRACT

A naphthalene sublimation technique is used to study the effect of surface injection on the mass (heat) transfer from a circular cylinder in crossflow. Using a heat/mass transfer analogy the results can be used to predict film cooling effects in the leading edge region of a turbine blade. Air injection through one row of circular holes is employed in the stagnation region of the cylinder. Streamwise and spanwise injection inclinations are studied separately, and the effects of blowing rate and injection location relative to the cylinder front stagnation line are investigated. Streamwise injection produces significant mass transfer increases downstream of the injection holes, but a relatively small increase is observed between holes, normal to the injection direction. The mass transfer distribution, measured with spanwise injection through holes located near the cylinder front stagnation line, is extremely sensitive to small changes in the injection hole location relative to stagnation. When the centers of the spanwise injection holes are located 5° or more from the stagnation line, the holes lay entirely on one side of the stagnation line and the injection affects the mass transfer only on that side of the cylinder, approaching the pattern observed with streamwise injection.

NOMENCLATURE

d	diameter of the test cylinder, 63.5 mm in present study
D	injection tube inner diameter, 5.95 mm
D_f	mass diffusion coefficient for naphthalene vapor in air; taking Sc = 2.5 (Sogin, 1958), $D_f = \nu/2.5$. [Note a more recent study by Chen (1987) indicates a smaller value of Sc and D_f. This would not affect the relative values of the mass transfer coefficient and Sherwood number with and without blowing.]
h	local convective heat transfer coefficient
h_o	reference mass transfer coefficient, $h_o = h_m$ without surface injection
h_H	adiabatic wall heat transfer coefficient for film cooling applications, $h_H = q_w/(T_w - T_{aw})$
h_m	local mass transfer coefficient, $h_m = \hat{m}/\bar{\rho}_{v,w}$
h'	isothermal wall heat transfer coefficient for film cooling applications, $h' = q_w/(T_w - T_1)$
h_o'	isothermal wall heat transfer coefficient for a situation where $\theta^* = 0$ (i.e., $T_2 = T_\infty$)
h_1'	isothermal wall heat transfer coefficient for a situation where $\theta^* = 1$ (i.e., $T_2 = T_w$)
H	shape factor, δ^*/δ_2
k	conductivity
L	length of test cylinder (also, height of the wind tunnel), 305 mm in the present study.
$\hat{m}$	local naphthalene mass transfer rate per unit area of the cylinder surface
M	blowing rate, $\rho_2 U_2/\rho_\infty U_\infty$
P_v	vapor pressure of naphthalene determined using the method by Ambrose, Lawrenson and Sprake, 1975.
$\bar{P}_v$	local vapor pressure of naphthalene at the cylinder surface averaged over the time of exposure in the wind tunnel
q_w	wall heat flux
R_n	gas constant for naphthalene (universal gas constant divided by molecular weight of naphthalene - 128.19)

* Now at the Mechanical Engineering Department of SUNY at Stony Brook, New York, 11794-2300.

Presented at the Gas Turbine and Aeroengine Congress and Exposition—June 4-8, 1989—Toronto, Ontario, Canada
This paper has been accepted for publication in the Transactions of the ASME
Discussion of it will be accepted at ASME Headquarters until September 30, 1989

s spanwise distance between centers of injection holes

t thickness of naphthalene layer

T temperature

T_o reference temperature

T_{aw} adiabatic wall temperature

T_r freestream recovery temperature

T_w wall temperature

T_2 film coolant temperature at the point of injection

T_∞ mainstream temperature

$\overline{T}$ local temperature of naphthalene surface averaged over exposure time in the wind tunnel

Tu turbulence intensity

U_2 mean velocity in injection tube

$\bar{U}_\infty$ mean velocity of mainstream

W width of test section

x direction along the tunnel test section

x' downstream distance from downstream edge of injection holes

y direction along the cylinder center line; $y = 0$, on the tunnel bottom wall

y' upward distance along the span of the cylinder measured from center of injection holes

z direction across the tunnel test section, $z = 0$, on the cylinder centerline

reek Symbol

α_i streamwise angle between the injection hole centerline and local cylinder surface, either 37° or 90° in this study

β_i spanwise angle between the injection hole centerline surface, either 20° or 90° in this study

δ^* displacement thickness of endwall boundary layer just upstream of the cylinder

Δt change in local naphthalene thickness due to exposure in the wind tunnel

$\Delta\tau$ time of cylinder exposure in wind tunnel

η film cooling effectiveness for an adiabatic wall, $\eta = (T_{aw} - T_\infty)/(T_2 - T_\infty)$

θ angle around the cylinder measured from the front stagnation point, degrees

θ_{inj} angular location of injection hole center relative to cylinder front stagnation point, degrees

θ^* dimensionless temperature, $\theta^* = (T_2 - T_\infty)/(T_w - T_\infty)$

μ dynamic viscosity of air

ν kinematic viscosity of air, μ/ρ

ρ density of air

ρ_s density of solid naphthalene, 1.145 gm/cm^3 (Karni, 1985)

$\rho_{v,i}$ density of naphthalene vapor at an inactive (non-subliming) surface, zero in this study

$\bar{\rho}_{v,w}$ local naphthalene vapor density on the cylinder surface averaged over exposure time in the wind tunnel

$\rho_{v,\infty}$ density of naphthalene vapor in the mainstream, zero in this study

Dimensionless Parameters

Nu local Nusselt number, hd/k

Re Reynolds number based on cylinder diameter, $U_\infty d/\nu$

Sc Schmidt number, ν/D_f

Sh local Sherwood number, $h_m d/D_f$

$\overline{Sh}_{sp}$ spanwise average Sherwood number at a given angle

INTRODUCTION

Application of film cooling through a single row or multiple rows of circular holes is common in gas turbine systems. The need to improve performance by increasing turbine inlet temperature, without shortening the components' lifespan, has prompted a large number of studies aimed at a better understanding of the complex flow and heat transfer mechanisms involved in film cooling (cf. Metzger, 1983). Advanced materials such as nickel super alloys and various ceramics which are used in modern turbines (Kear, 1986) have, in general, relatively low thermal conductivity and diffusivity. Thus, large local variations of the heat transfer coefficient can produce significant temperature gradients in the wall of a turbine blade. These gradients may cause high thermal stresses and ultimately could lead to blade failure. An effective film cooling design must reduce the temperature gradients over the surface, as well as the mean wall temperature. Therefore, knowledge of the heat transfer distribution over the blade surface, with various coolant injection configurations, is necessary for a successful turbine design.

Two methods have been developed to predict film cooling effects on heat transfer. The first method (Eckert, 1983 and Goldstein, 1971) defines the heat transfer coefficient with an adiabatic wall temperature

$$q_w = h_H(T_w - T_{aw}) \qquad (1)$$

For a constant property flow, the heat transfer coefficient h_H is independent of the temperature difference $T_w - T_{aw}$. A dimensionless adiabatic wall temperature, known as the film cooling effectiveness, η, is given by:

$$\eta = \frac{T_{aw} - T_r}{T_2 - T_r}$$

For low-speed constant property flows, $T_r = T_\infty$

$$\eta = \frac{T_{aw} - T_\infty}{T_2 - T_\infty} \qquad (2)$$

In this method, the heat transfer coefficient and the effectiveness are determined separately. Then, for any given mainstream and coolant temperatures and a prescribed wall heat flux, the wall temperature distribution can be obtained using Eq. (1).

In the second method (Metzger et al., 1968 and Choe et al., 1974) the heat transfer coefficient is defined by the equation

$$q_w = h'(T_w - T_\infty) \qquad (3)$$

This approach provides a direct means of determining heat transfer coefficients for film cooling on an isothermal surface. Here, the heat transfer coefficient h' is not independent of the temperature difference $T_w - T_\infty$; but as shown in Metzger et al., 1968, Metzger and Fletcher, 1971, and Eckert et al., 1971, for a constant property flow, h' varies linearly with the dimensionless temperature

$$\theta^* = \frac{T_2 - T_\infty}{T_w - T_\infty} \qquad (4)$$

Note that unlike h_H, the coefficient h' - defined by Eq. 3 - can take on unusual (e.g. negative) values, especially close to an injection location. The coefficients h_0' and h_1' obtained on an isothermal surface for $\theta^* = 0$ and 1, respectively, can be used to approximate heat transfer coefficients on a surface where gradual temperature variations take place (Eckert, 1983). In that case,

$$h_0' \approx h_H \qquad (5)$$

and the relation between h' and θ^* is given by

$$\frac{h'}{h_H} = 1 - \eta\theta^* \qquad (6)$$

In various studies (Metzger and Fletcher, 1971, Miller and Crawford, 1984, and Ligrani and Camci, 1985) values of h_H and η were approximated from h' and θ^* data using a linear extrapolation based on Eq. (6).

Values of the heat transfer coefficient h_H for two-dimensional slot injection across the span of a flat plate are presented by Hartnett, Birkebak and Eckert, 1961a and 1961b. Their data show relatively large coefficients near the injection slot; as the downstream distance from the slot increases, h_H quickly declines approaching the coefficient obtained without injection. Measurements of heat transfer coefficients averaged across the test surface are reported in some studies of three-dimensional film cooling from a single row and multiple rows of circular holes (Metzger and Fletcher, 1971; Mayle and Camarata, 1975; Liess, 1975; Metzger, Kuenstler and Takeuchi, 1976; Lander, Fish and Suo, 1972; Ligrani and Breugelmans, 1981). Effects of parameters such as injection geometry, blowing rate, pressure gradient, and boundary layer transition on variation of spanwise-averaged coefficients in the mainflow direction were investigated in these studies.

Local heat transfer coefficients (h_H) over a film-cooled plate with one and two rows of injection holes were measured by Eriksen and Goldstein, 1974 and Jabbari and Goldstein, 1978. Mick and Mayle (1988) measured local h_H values using two rows of spanwise injection holes located 15° and 44° from the stagnation line of a blunt body with a circular leading edge, followed by a flat section. Local measurements near the leading edge of a turbine vane and on the front portion of a cylinder were conducted at Purdue University by Hanus and L'Ecuyer, 1977; Luckey, Winstanley, Hanus and L'Ecuyer, 1977; Luckey and L'Ecuyer, 1981; and Bonnice and L'Ecuyer, 1983. In these studies h' values were obtained near the center of the wind tunnel (cylinder mid-span). Spanwise injection through one to five rows of holes was employed.

In an experimental set-up where significant temperature differences exist (Ericksen et al., 1974; Jabbari et al., 1978; Mick et al., 1988; Hanus et al., 1977; Luckey et al., 1977; Luckey et al., 1981; and Bonnice et al., 1983) wall conduction makes it difficult to maintain the imposed boundary condition (T_w = constant or q_w = constant) near the injection holes and close to the edges of the test surface. Consequently, in several studies the analysis between heat and mass transfer was utilized to obtain transfer coefficients on flat surfaces (Hay, Lampard and Saluja, 1985a; Hay Lampard and Saluja, 1985b; Goldstein and Taylor, 1982; and Kumada, Hirata and Kasagi, 1981). The last two studies demonstrated how mass transfer using naphthalene sublimation can provide contours of local transfer coefficients on a flat plate near the holes of single-row and multiple-row injection geometries.

When naphthalene sublimation is used, a direct analogy to the adiabatic wall heat transfer coefficient (h_H) defined by Eq. (1) leads to the following definition of a mass transfer coefficient:

$$h_m = \frac{\dot{m}}{(\bar{\rho}_{v,w} - \rho_{v,i})} \qquad (7)$$

Alternatively, an equivalent relation to Eq. (3), gives

$$h_m = \frac{\dot{m}}{(\bar{\rho}_{v,w} - \rho_{v,\infty})} \qquad (8)$$

In the naphthalene sublimation technique used in the present study a nearly-uniform vapor density is maintained over the entire cylinder surface, and the naphthalene vapor concentration in the mainstream and in the injected gas is zero. This is equivalent to isothermal boundary conditions with $T_2 = T_\infty$ (or $\theta^* = 0$). Thus, Eqs. (7) and (8) both reduce to

$$h_m = \frac{\dot{m}}{\bar{\rho}_{v,w}} \qquad (9a)$$

In the present study local mass transfer coefficients are obtained around the entire circumference of a circular cylinder and along a span containing five injection holes (in a single row). Spanwise and streamwise inclined injections are employed at blowing rates of 0.5, 1.0 and 2.0. The injection location is varied relative to the cylinder's front stagnation line. In each test run, measurements are taken at about 3800 local points over the cylinder surface. Thus, exact details of the mass transfer distribution pattern are revealed. Injection geometry and blowing rate effects in the region away from the

base of the cylinder - where endwall effects on the flow are relatively small - are reported here. The injection effects near the endwall will be reported later.

EXPERIMENTAL APPARATUS AND MEASUREMENT TECHNIQUES

The primary objective of the experimental apparatus is to provide a means of determining the local rate of naphthalene sublimation from the cylinder surface during exposure to an air flow. This local mass transfer rate is then expressed in terms of the coefficient h_m and the Sherwood number. Detailed descriptions of the experimental apparatus and the measurement procedure are given by Karni, 1985. The maximum measurement error in obtaining h_m is 6%.

The test cylinder (d = 63.5 mm) is shown in Fig. 1; a portion extending over about 60° of the cylinder circumference and along its entire naphthalene-covered span is removed [see Fig. 1(a)] and two sections with different injection inclinations are made to fit in that region [Figs. 1(b) and 1(c)]. During tests the cast naphthalene layer covers the outer surface of the section used as if it were an integral part of the cylinder. Teflon (Polytetra-Fluoro-Ethylene) injection tubes are installed in these sections; in one section, the tubes are inclined such that the injected air enters the mainstream at a spanwise angle of 20° to the cylinder surface [Fig. 1(b)]; in the other section, the tubes are angled 37° to the surface in the streamwise direction [Fig. 1(c)]. All injection tubes have an inside diameter of 5.95 mm and a wall thickness of 0.35 mm. They extend 1.0 mm out of the section surface and thus are flush with the naphthalene layer outer surface. The injection holes extend over an angular range of 18° and 10.5° of the cylinder circumference for streamwise and spanwise injection, respectively. If the injection tube's wall thickness is included, these angles become 20° and 12°, respectively. The ratio of cylinder diameter to injection hole diameter (d/D = 10.67) is similar to that used in the leading edge of many turbine vanes. The hole diameter is of the same order of magnitude as the cylinder boundary layer (cf. Karni, 1985).

During its exposure to the air stream, the test cylinder is positioned vertically in the middle of the tunnel's cross section, about 450 mm downstream of the test section inlet; the blockage ratio is 0.104. The naphthalene-covered portion of the cylinder extends from about 6.7 mm below the tunnel's bottom wall to 260 mm above it (about 45 mm below the top wall). The secondary (injected) air flow is supplied by a compressor. To insure a steady flow of dry air in the injection system, the secondary air is filtered and passes through two flow regulators. It then flows through a calibrated orifice and a temperature-control device. The difference between the mainstream and secondary air temperatures is within 0.25°C in all test runs. To prevent flow rate variations from one injection hole to another, the secondary air enters the test cylinder (d = 63.5 mm) through a long narrow slit cut along the span of 25.4 mm O.D. aluminum tube. This tube is attached to the secondary air line on one end and is sealed on the other. It is mounted inside the test cylinder, extending over most of its span. The uniformity of the injected air flow rate was verified experimentally (Karni, 1985).

The time of exposure in the wind tunnel ($\Delta\tau$) is between 35 and 70 minutes (depending on operating conditions). During tests 0.020-0.13 mm of naphthalene sublime from the cylinder surface. Since the mainstream and the injected air contain no naphthalene vapor, the local mass transfer coefficient is

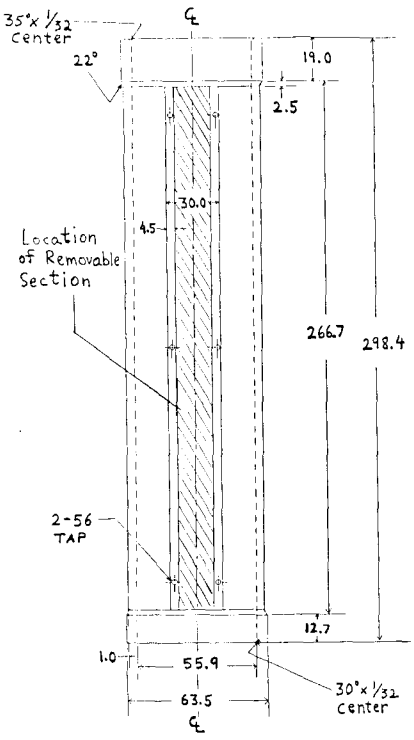

Fig. 1(a) The test cylinder without the removable section (dimensions in millimeters)

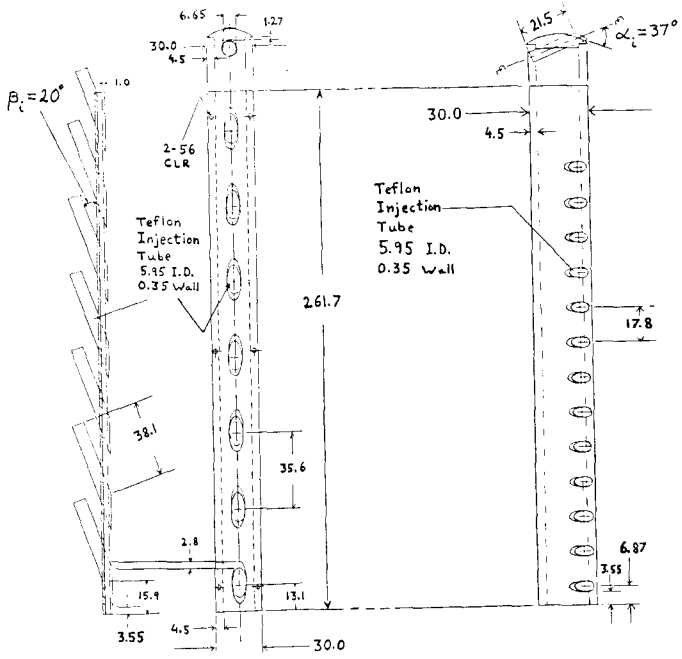

Fig. 1(b) A removable section with spanwise injection holes (dimensions in millimeters)

Fig. 1(c) A removable section with spanwise injection holes (dimensions in millimeters)

$$h_m = \frac{\dot{m}}{\bar{\rho}_{v,w}} = \frac{\rho_s \Delta t/\Delta\tau}{\bar{\rho}_{v,w}} \qquad (9b)$$

where

$$\bar{\rho}_{v,w} = \frac{\bar{P}_v}{R_n \bar{T}} \qquad (10)$$

The results can be expressed in terms of the local Sherwood number,

$$Sh = \frac{h_m d}{D_f} \qquad (11)$$

OPERATING CONDITIONS

The various operating conditions are specified in Table 1. In all the test runs, the freestream velocity and the Reynolds number are within 2% of the values given in the table. The mainstream turbulence intensity is measured while the cylinder is out of the wind tunnel.

In all the tests, measurements are conducted over a span containing 5 injection holes (including the region immediately above the endwall) and around the entire cylinder circumference. Spanwise injection is directed toward the endwall.

TABLE 1
OPERATING CONDITIONS

Freestream	Endwall Boundary Layer
$Re_d \cong 76{,}000$	$\delta^* \cong 2.23$ mm
$U_\infty \cong 19.16$ m/s	$\delta_2 \cong 1.56$ mm
$Tu \cong 0.45\%$	$H \cong 1.43$

cylinder diameter, d = 63.5 mm
injection hole diameter, D = 5.95 mm
blockage ratio, d/W = 0.104
aspect ratio, L/d = 4.8

Streamwise Injection			Spanwise Injection		
α_j=37°	β_j=90°	s/D=3	α_j=90°	β_j=20°	s/D=6
M	θ_{inj}(degrees)		M	θ_{inj}(degrees)	
0.50	10		0.50	1	
0.50	20		0.51	3	
0.50	30		0.50	5	
1.01	10		0.99	2	
1.02	10[1]		1.00	3	
1.01	20		1.01	3[1]	
1.00	30		0.99	7	
1.99	10		2.00	0	
2.01	20		2.01	1	
1.99	30		1.99	5	

[1]Test runs where the lower edge of the first injection hole is located 1.0 hole-diameter above the endwall. In all the other tests, the lower side of the first injection hole is adjacent to the tunnel bottom wall.

RESULTS

1. Streamwise Injection

The Sherwood number distributions for a streamwise injection angle, α_j, of 37°, an injection locations θ_{inj} of 10° and blowing rate M of 0.50, 1.0 and 2.0, are shown in Figs. 2(a), (b) and (c), respectively. These (and all other) computer-drawn contour plots are obtained from the actual measurements around the entire cylinder circumference and over part of its span. The difference between adjacent contour lines corresponds to a Sh change of 200. The injection holes are shown by the shaded regions in the left-hand side of each figure. Since the measurement points located nearest each hole are not evenly distributed around its periphery, the contour lines very near the holes are somewhat distorted during the computer drawing process and do not follow the exact shape of the hole where Sh = 0.

Figure 2 demonstrates that the injected air jets produce large Sh values and steep local gradients downstream of the injection holes while a relatively small increase in Sh is seen between the holes. The contours clearly indicate the flow pattern near the injection holes. Somewhat similar mass transfer trends were reported in studies of streamwise injection over flat plates by Hay et al., 1985a; Kumada et al.,1981; and Goldstein et al., 1982. In Goldstein et al., 1982 larger increases of Sh were observed between injection holes on a flat plate. The present data show that the region downstream of each hole, where the injected flow has a relatively large effect increases with increasing blowing rate, but is generally limited to the front

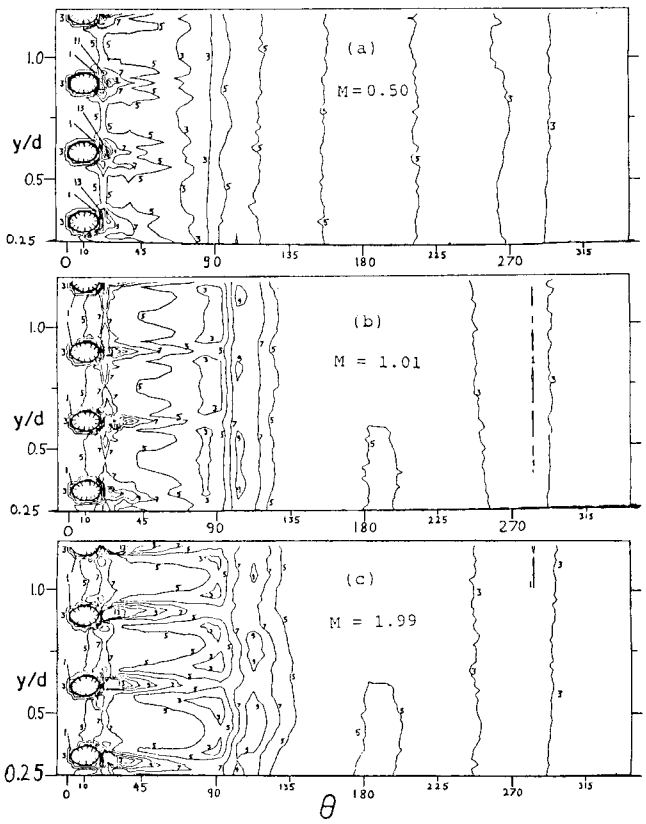

Fig. 2 Sh distribution for streamwise injection. Contours of Sh x 10^{-2}, α_j = 37°; β_j = 90°; θ_{inj} = 10°; s/D = 3

portion of the cylinder. A symmetric Sh distribution is observed downstream of holes located at y/d > 0.5, but the spanwise pressure gradients, created by the endwall boundary layer in the cylinder's front stagnation region, divert the jets of the lower injection hole toward the tunnel wall.

Figure 3 shows angular variations of Sh at selected spanwise distances from the center of an injection hole located far from the endwall for α_j = 37°, M = 0.50, and θ_{inj} = 10°. The circumferential Sh distribution measured over a cylinder with no injection holes is also shown in this figure. The spanwise distance from the hole's center is denoted by y'. The location of a given y' with respect to the injection hole is shown in the insert at the top right corner of Fig. 3. Immediately downstream of the hole's centerline (y'/D = 0), Sh is more than 3 times its value without injection. As y'/D and/or θ increase, Sh decreases sharply. Figures 2 and 3, show that Sherwood number values measured upstream of an injection hole's centerline and on the opposite side of the cylinder symmetry line are nearly unaffected by the injected jets; the mass transfer pattern in these regions is similar to that measured by Karni, 1985 over a cylinder with no injection holes.

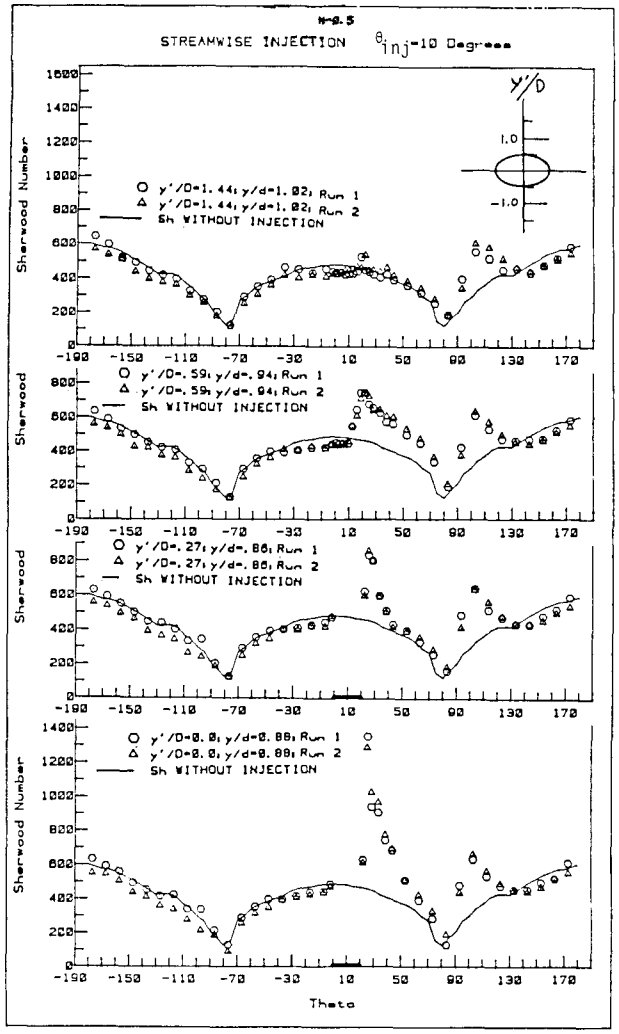

Fig. 3 Angular variations of Sh at slected spanwise distances from the center of an injection hole M = 0.50; α_j = 37°; θ_{inj} = 10°

Variations of spanwise average Sherwood number, $\overline{Sh}_{sp}$, around the cylinder for α_j = 37° are presented in Fig. 4. The Sh distribution obtained far from the endwall on a cylinder with no injection holes is also shown in this figure. The spanwise-averaged coefficients confirm the trends seen in Figs. 2 and 3 (local Sh distributions). Maximum Sh value showing an increase of 2 - 3 times over the mass transfer without injection are observed immediately downstream of the injection holes. In the region most influenced by injection (θ_{inj} < θ < 120°), $\overline{Sh}_{sp}$ values located immediately downstream of injection fall sharply as θ increases, reaching a minimum near the laminar boundary layer separation angle (θ ≈ 80°-90°); a second peak is observed at θ = 110° - 120°. At 80° < θ < 180°, $\overline{Sh}_{sp}$ has a pattern similar to a Nu(Sh) distribution over an impermeable circular cylinder at critical and supercritical Re_d (Schmidt and Wenner, 1941; Giedt, 1949; Achenbach, 1975; and Sogin and Subramanian, 1961) At high Reynolds numbers (Re_d > 2x10^5), the down-

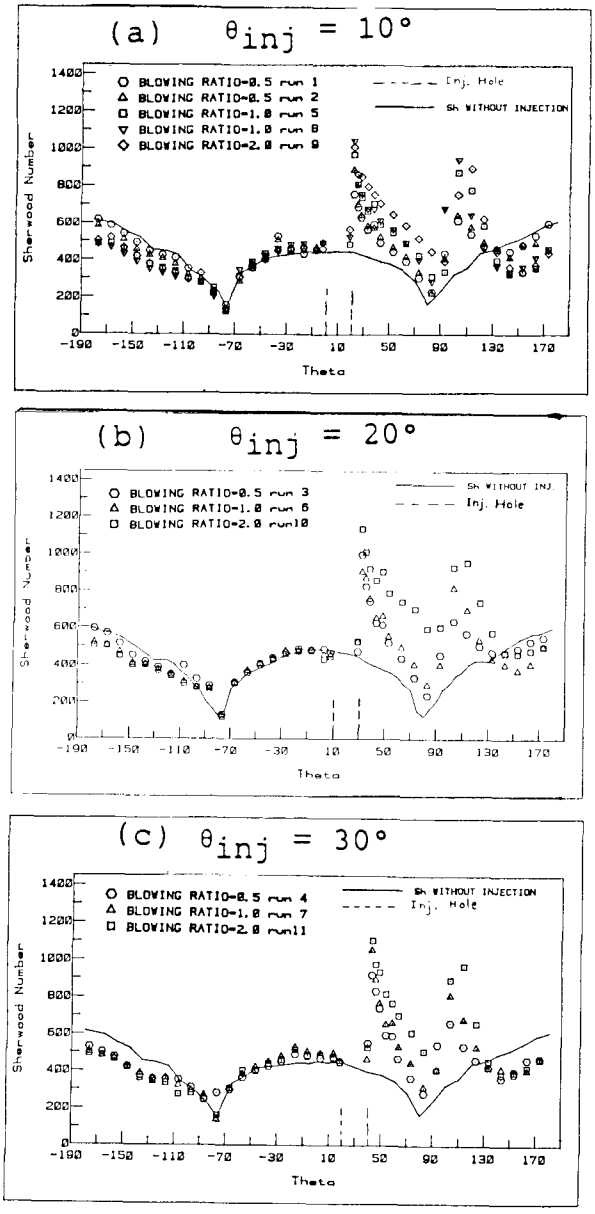

Fig. 4 Spanwise average Sherwood number distribution for streamwise injection. α_j = 37°; β_j = 90°; s/D = 3

stream portion of the cylinder boundary layer becomes turbulent producing a sharp increase of heat (mass) transfer, and the separation angle is between 110° and 150°. It is possible that the additional momentum supplied by the jets causes a delay in the boundary layer separation, and over some portions of the cylinder span a transitional or turbulent boundary layer exists at $\theta \approx 90° - 130°$.

Figure 4 shows that on the side of the cylinder where no injection is employed ($\theta < 0°$) $\overline{Sh}_{sp}$ is similar to the impermeable wall coefficient over the front of the cylinder; but, for M = 1.0 and 2.0, $\overline{Sh}_{sp}$ is somewhat lower than this coefficient in the wake region. At $\theta_{inj} = 30°$, relatively low $\overline{Sh}_{sp}$ values are obtained in the wake for M = 0.5 as well. This may be caused by the jets' interference with the characteristic wake pattern of alternating vortex shedding. Note that similar reductions of heat (and mass) transfer were measured in the wake of a smooth impermeable cylinder exposed to a mainstream with high turbulent intensity, (Kestin and Wood, 1971, and Lowery and Vachon, 1975), and when a splitter plate was installed at $\theta = 180°$ (Hiwada, Niwa, Kumada and Mabuchi, 1979).

II. Spanwise Injection

The investigation of spanwise injection focuses on the influence of small variations in θ_{inj} near the cylinder front stagnation line at different blowing rates. As in Fig. 2 all computer-drawn contour plots (Figs. 5 and 6) are prepared via interpolations of the actual measurements. The injection holes (which, in these figures, are divided into two parts) are indicated by the shaded regions near the left and right boundaries of the figures. Note that the injected jets are directed toward the endwall.

Sherwood number distributions for an injection angle, β_j, of 20°, a blowing rate, M, of about 0.5, and injection locations, θ_{inj} of 1°, 3° and 5° are presented in Figs. 5(a), (b) and (c), respectively. Note that based on their inner diameter, the maximum angular range of the holes is about 10° ($\theta_{inj} \pm 5°$); thus, at $\theta_{inj} = 5°$, the injection holes are entirely on one side of the cylinder stagnation line. A nearly symmetric (around $\theta = 0$) Sh distribution is seen in Fig. 5(a) ($\theta_{inj} = 1$) as θ_{inj} increases to 3° [Fig. 5(b)] and to 5° [Fig. 5(c)], the injection effects become skewed. Although the jets are injected with a relatively large spanwise velocity component ($\beta_j = 20°$) and a zero streamwise component ($\alpha_j = 90°$), they appear to be turned downstream by the main flow immediately upon their entry when $\theta_{inj} = 3°$ or 5° [Fig. 5(b) and (c)]. Consequently the mass transfer pattern approaches that observed with streamwise injection (Fig. 2). Mick and Mayle (1988) observed a similar pattern while employing two rows of injection holes at $\beta_j = 30°$ and $\theta_{inj} = 15°$ and 44°. In Figs. 5(a,b,and c) low transfer coefficients are seen along the cylinder span at $\theta \approx 80°$, and local Sh peaks are detected at $\theta \approx 100°$ to 110°.

Sherwood number distributions for $\beta_j = 20°$, $M \approx 2.0$, and $\theta_{inj} = 0°$ and 5° are presented in Figs. 6(a) and (b) respectively. A symmetric Sh distribution is seen over both sides of the cylinder stagnation line for $\theta_{inj} = 0°$ [Fig. 6(a)], but the Sh distribution is quite skewed at $\theta_{inj} = 5°$ [Fig. 6(b)]. However, at M = 2.0 and $\theta_{inj} = 5°$ [Fig. 6(b)] the jet trajectories retain larger downward spanwise components after entering the main flow than do their counterparts at m = 0.5 [Fig. 5(c)]. The skewed distribution obtained at all blowing rates for $\theta_{inj} \leq 5°$ probably result from the entire hole cross-section being located on one side of the cylinder front stagnation line. Thus, the other

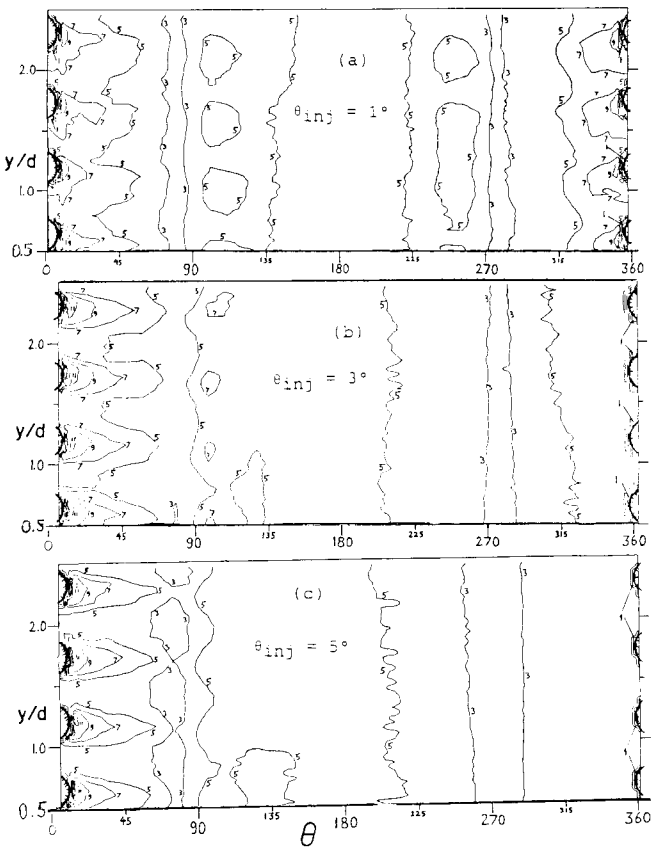

Fig. 5. Sh distribution for spanwise injection. Contours of Sh x 10^{-2}. M = 0.50; α_j = 90°; β_j = 20°; s/D = 6

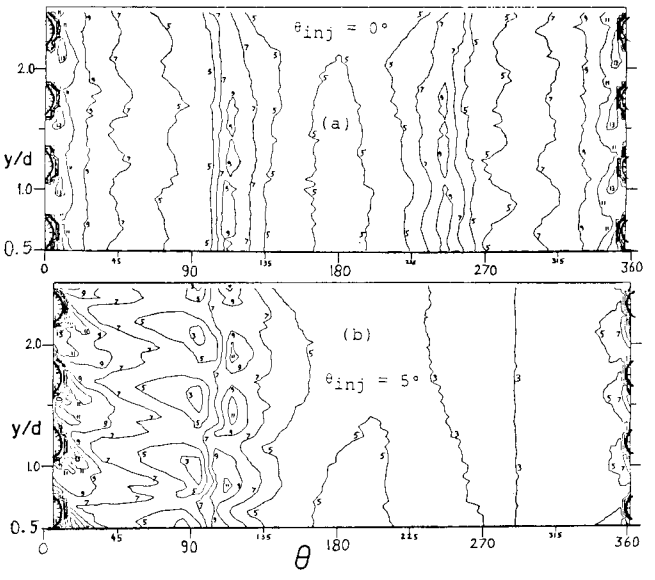

Fig. 6. Sh distribution for spanwise injection. Contours of Sh x 10^{-2} M = 2.00; α_j = 90°; β_j = 20°; s/D = 6

side of this line is unaffected by injection at M = 0.5 and 1.0, and only modest increases over a small region are seen at M = 2.0. For M ≈ 2.0 (Fig. 6), relatively low Sh values are detected at θ = 90° - 100°, and local highs are seen at θ = 110° - 115°. Especially large Sh variations occur at 80° < θ < 120° when θ_{inj} = 5° is employed [Fig. 6(b)].

Figure 7 shows angular variations of Sh at selected spanwise distances from the center of an injection hole located far from the endwall for M ≈ 1.0, β_j = 20°, and θ_{inj} = 3°. The relation between the distance from the hole's center (y') and the injection hole is shown in the insert at the top of the figure. These data show that as the downward distance from the hole's center increases, the injection effect increases on both sides of the hole. Maximum Sh values of about 2.5 times that without injection are observed adjacent to the holes and just below them.

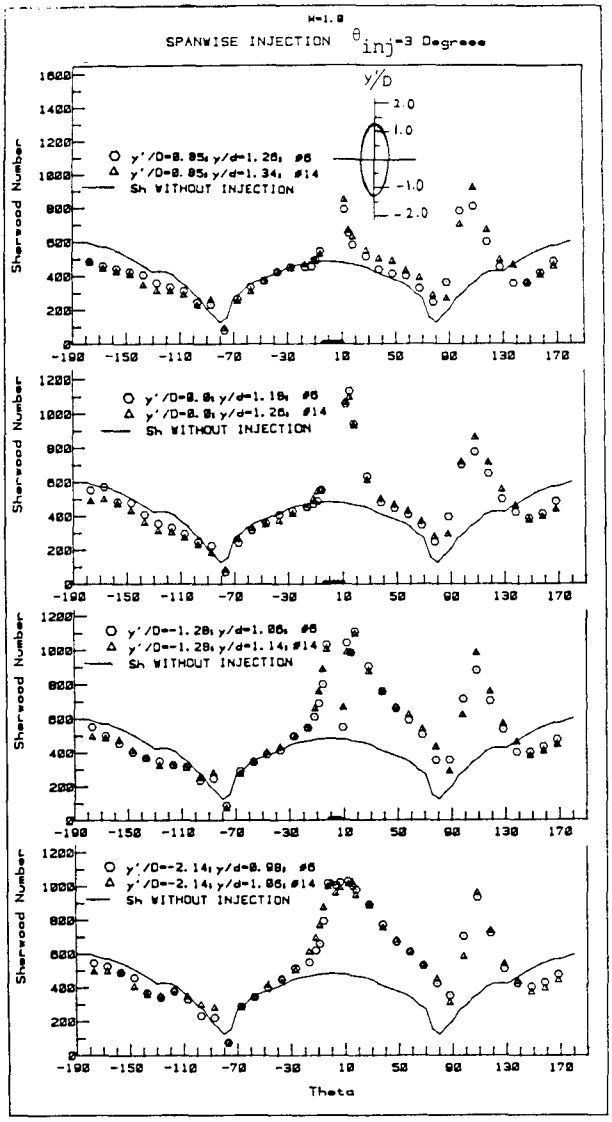

Fig. 7 Angular variations of Sh at selected spanwise distance from the center of an injection hole M = 0.99; β_j = 20°; θ_{inj} = 3°

Spanwise average Sherwood number ($\overline{Sh}_{sp}$) values are presented in Fig. 8. The circumferential Sh distribution obtained far from the endwall on a cylinder with no injection holes is also shown in these figures. The spanwise-averaged coefficients show some of the trends seen in Figs. 5-7 (local Sh distributions). The Sh peaks near the injection holes increase with the blowing rate and are 2 - 3 times the Sh value without injection. For a given blowing rate, $\overline{Sh}_{sp}$ on the side of the cylinder's stagnation line opposite to injection (in the angular range -130° < θ < 0°) drops sharply as θ_{inj} increases (approaching an impermeable wall distribution, whereas $\overline{Sh}_{sp}$ values on the injection side (at θ_{inj} < θ < 130°) are nearly unaffected by changes in the injection location. The last observation is surprising, considering the great influence of small θ_{inj} variations on local Sh distribution (Figs. 5-6) and the fact that the bulk mass flow over the injection side increases as θ_{inj} increases while the bulk flow

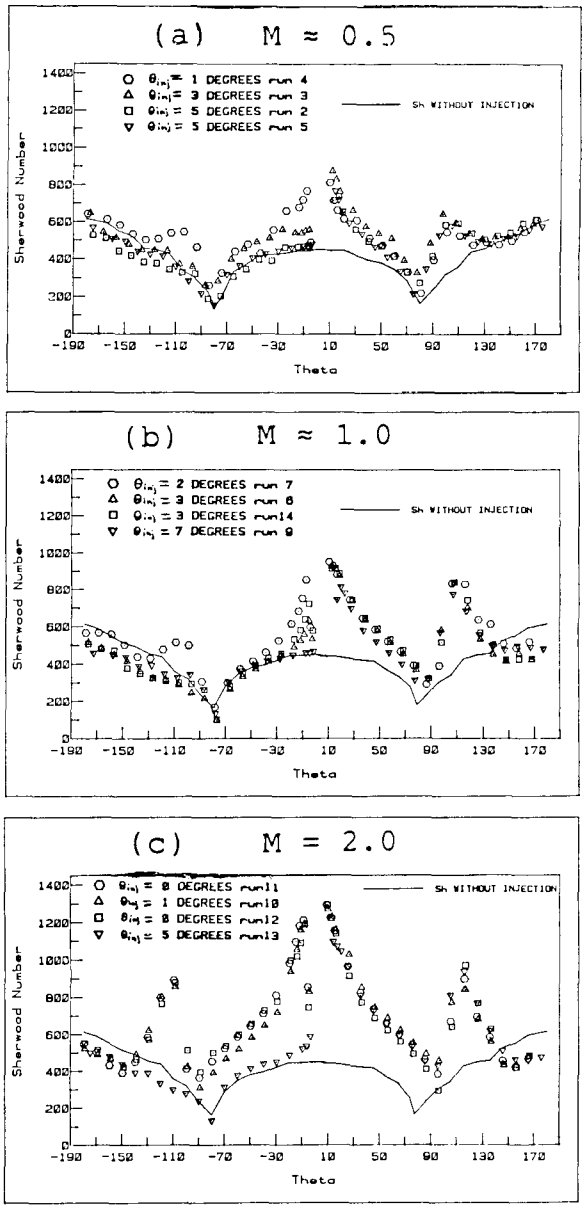

Fig. 8 Spanwise average Sherwood number distribution for spanwise injection. α_j = 90°; β_j = 20°; s/D = 6

over the other side decreases. For θ_{inj} = 5° - 7°, the $\overline{Sh}_{sp}$ values on the side opposite to injection closely follow the impermeable wall distribution in the angular range -90° < θ < 0° (Fig. 8). The average coefficients on the injection side (or both sides for 0° ≤ θ_{inj} ≤ 3°) peak immediately downstream of injection and fall sharply as θ increases. A minimum $\overline{Sh}_{sp}$ is reached between θ = 80° and θ = 100°, depending on blowing rate. A second peak is observed at θ = 100° - 120°, and further downstream, $\overline{Sh}_{sp}$ decreases, approaching values comparable to those obtained without injection. Similar to average coefficients for streamwise injection (Fig. 4), the $\overline{Sh}_{sp}$ distribution at 90° < θ < 180° for spanwise injection (Fig. 8) resembles a circumferential distribution over the rear portion of an impermeable cylinder at critical and supercritical Re_d, (Schmidt et al., 1941; Giedt, 1949; Achenbach, 1975; and Sogin et al., 1961). For all injection locations, at M = 2.0 $\overline{Sh}_{sp}$ values in the downstream portion of the wake (θ = 180° ± 50°) are lower than the impermeable wall distribution [Fig. 8(c)]. This is also true at lower blowing ratios when $\theta_{inj} \geq 3°$ [Figs. 8(a) and (b)]. Local Sh data in Fig. 7 show the same trend in the wake as that mentioned above; it may result from the fact that the injected jets interfere with the symmetrical vortex shedding pattern which is characteristic to a cylinder in crossflow.

III. Comparison of Results

Figure 9 presents spanwise-averaged Sherwood number ($\overline{Sh}_{sp}$) distributions for streamwise and spanwise injection at M ≈ 1.0 and θ_{inj} = 10° and 7° respectively. The $\overline{Sh}_{sp}$ distributions obtained with the two injection geometries are similar despite the fact that at a given blowing rate, the total injected mass flow for streamwise injection (s/D = 3; 13 holes) is nearly twice that of spanwise injection (s/D = 6; 7 holes).

Heat transfer measurements over a film-cooled circular cylinder were conducted by Bonnice and L'Ecuyer (1983). A comparison between their data and present results for spanwise injection at similar geometry is given in Figs. 10(a) and (b). Figure 10(a) shows local h/h_o values directly downstream of an injection hole (y'/D = 0). Figure 10(b) shows spanwise average $\bar{h}/h_o$ values. Table 2 details the geometry used in both studies to obtain the data shown in these figures.

The linear extrapolation approach, commonly used to approximate h'_o (= h_H) values from h' measurements at θ^* larger than zero (Choe et al., 1974; Metzger et al., 1971; Miller et al., 1984; and Ligrani et al., 1985), is used to obtain h'_o/h' from the data of Bonnice and L'Ecuyer, 1983. Note that only two (relatively close) θ^* values were used in Bonnice and L'Ecuyer, 1983, (1.03 and 1.29). Thus, the extrapolated h'_o/h' values may be inaccurate. (Any error in the measurements or the calculations is magnified by a factor of about 4.0 when h' values at θ^* = 1.03 and 1.29 are extrapolated to give h'_o).

As shown in Table 2, the main difference between the present injection geometry and that of Bonnice and L'Ecuyer, 1983 is the ratio of cylinder to injection hole diameter, d/D. Thus, for a given x'/D, their data points are, in fact, at a much smaller angular distance θ_{inj} than present data. This may account for the somewhat different h/h_o patterns obtained in the two studies at y'/D = 0.0 [Fig. 10 (a)]. The fact that larger injection holes are used in the present study implies that, at a given blowing rate, the total injected mass flow in present tests is higher than that of Bonnice and L'Ecuyer, 1983. Thus, their average values $\bar{h}/h_o$ at M = 2.0 agree better with present data at M = 1.0 than at M = 2.0 [Fig. 10(b)].

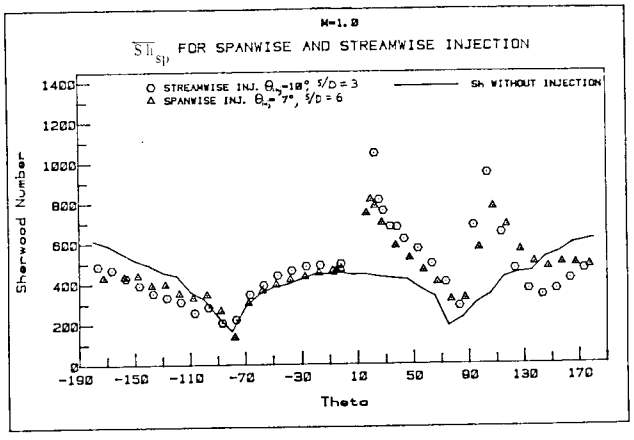

Fig. 9 Comparison of $\overline{Sh}_{sp}$ for streamwise and spanwise injection. M = 1.0; θ_{inj} = 7° - 10°

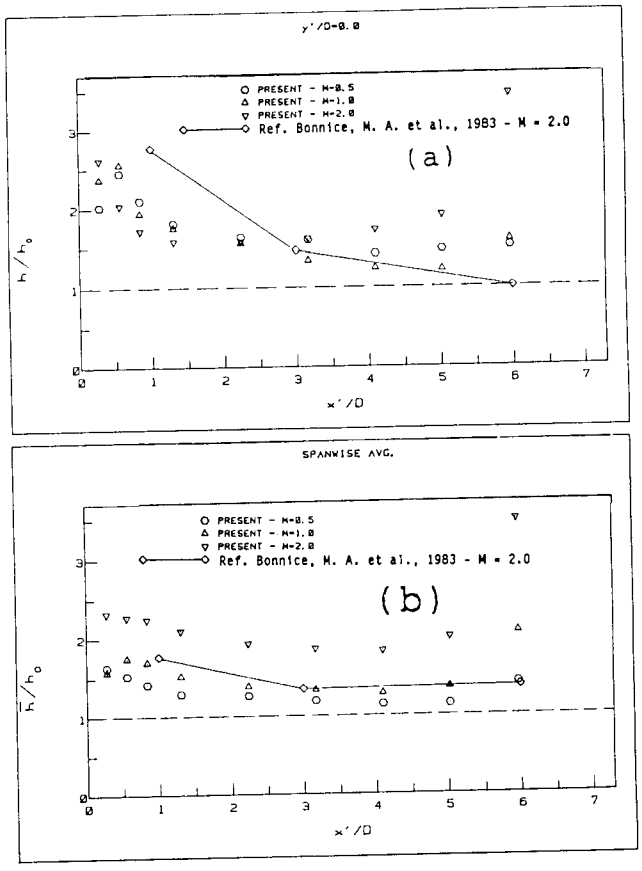

Fig. 10(a) Comparison of local mass transfer downstream of a spanwise injection hole with extrapolated data from Bonnice et al., 1983. y'/D = 0.0; θ_{inj} = 5° - 7°

Fig. 10(b) Comparison of $\overline{Sh}_{sp}$ for Spanwise injection with extrapolated data from Bonnice et al., 1983, θ_{inj} = 5° - 7°

TABLE 2
SPANWISE INJECTION GEOMETRY
FOR DATA SHOWN IN FIG. 12

	Cylinder Diameter (mm)	Injection Tube Diameter (mm)	d/D	s/D	β_i	θ_{inj}	θ^*
Present	63.5	5.95	10.67	6	20°	5°,7°	0
Bonnice, & L'Ecuyer, (1983)	150	4.76	31.5	5	25°	5°	1.03 1.29

CONCLUSIONS

Several surface injection parameters affecting mass transfer from a circular cylinder (or a turbine vane leading edge) have been investigated. The following conclusions may be drawn from the results obtained with spanwise and streamwise injection holes at angular locations of 0° to 7° and 10° to 30° from stagnation, respectively, and at blowing rates of 0.5 to 2.0.

a) The injected jets produce large Sh values and steep local gradients downstream of the streamwise injection holes while a relatively small increase in Sh is detected between the holes. A somewhat similar periodic pattern, corresponding to individual jet trajectories, is also observed for spanwise injection when the holes are located entirely on one side of the cylinder stagnation line (i.e., $\theta_{inj} \geq 5°$). For such geometries, the injection effects on the opposite side of the stagnation line are relatively very small.

b) For streamwise injection, the size of the region directly downstream of each hole, where high Sh values are found, increases with M and decreases as the injection is shifted downstream (i.e., as θ_{inj} increases).

c) The local mass transfer distribution for spanwise injection near the stagnation line is extremely sensitive to small variations in θ_{inj}. Nearly symmetric Sh distributions are obtained for θ_{inj} = 0° - 1°, but, for θ_{inj} of 3°or higher, the injection effects become very skewed. Despite that, the spanwise-averaged coefficients over the side of the stagnation line where injection is employed vary little with θ_{inj}. $\overline{Sh}_{sp}$ does, however, approach the values for a cylinder without injection on the other side of the symmetry line as θ_{inj} increases.

d) For both streamwise and spanwise injections, Sh values generally decrease with downstream distance from injection, reaching a minimum at θ = 80° - 100°. Further downstream, local peaks are observed at θ = 100° - 120°. This trend could result from a boundary layer transition to turbulence, which may occur over portions of the cylinder span at θ = 80° - 90°.

e) Mass transfer values lower than those obtained with a uniform cylinder are observed in the downstream portion of the wake (θ = 180° ± 50°) for streamwise injection at M = 1.0 and 2.0. A similar pattern is seen with spanwise injection at M = 2.0 and, if θ_{inj} is between 3° and 7°, at M = 1.0, also. This trend is probably due to the injected jets interfering with the characteristic wake pattern of alternate vortex shedding.

f) Downstream of injection, the spanwise-averaged Sherwood number generally increases with blowing rate.

REFERENCES

Achenbach, E. "Total and Local Heat Transfer from a Smooth Circular Cylinder in Cross-Flow at High Reynolds Number," Int. J. Heat Mass Transfer, 18, 1387-1396 (1975).

Ambrose, D., I.J. Lawrenson, and C.H.S. Sprake. "The Vapor Pressure of Naphthalene," J. Chemical Thermodynamics, 7, 1173-1176 (1975).

Bonnice, M.A., and M.R. L'Ecuyer, "Stagnation Region Gas Film Cooling - Effects of Dimensionless Coolant Temperature," NASA CR-168197 (1983).

Chen, P.H., "Measurement of Local Mass Transfer from a Gas Turbine Blade," Ph.D. Thesis, University of Minnesota, January 1988.

Choe, H., W.M. Kays, and R.J. Moffat. "The Superposition Approach to Film Cooling," ASME Paper No. 74-WA/HT-27 (1974).

Eckert, E.R.G., "Analysis of Film Cooling and Full Coverage Film Cooling of Gas Turbine Blades," ASME Paper No. 83-GTJ-2 (1983).

Eckert, E.R.G., R.J. Goldstein, and D.R. Pedersen. "Comment on 'Evaluation of Heat Transfer for Film-Cooled Turbine Components,'" J. Aircraft, 8, 63-64 (1971).

Eriksen, V.L., and R.J. Goldstein. "Heat Transfer and Film Cooling Following Injection Through Inclined Circular Tubes," J. Heat Transfer, 96,

Giedt, W.H. "Investigation of Variation of Point Unit Heat Transfer Coefficient Around a Cylinder Normal to an Air Stream," Trans. ASME, 71, 375-381 (1949).

Goldstein, R.J. "Film Cooling," in Advances in Heat Transfer, Vol. 7, pp. 321-379. T.F. Irvine and J.P. Hartnett, eds. New York: Academic Press (1971).

Goldstein, R.J., and J.R. Taylor. "Mass Transfer in the Neighborhood of Jets Entering a Crossflow," J. Heat Transfer, 104, 715-721 (1982).

Hanus, G.J., and M.R. L'Ecuyer. "Leading-Edge Injection for Film Cooling of Turbine Vanes," AIAA Journal of Energy, 1(1), 44-49 (1977).

Hartnett, J.P., R.C. Birkebak, and E.R.G. Eckert. Effectivenss and Heat Transfer in Cooling of a Surface with a Pressure Gradient," in International Developments in Heat Transfer, Part IV, pp. 682-689. New York: American Society of Mechanical Engineers (1961a).

Hartnett, J.P., R.C. Birkebak, and E.R.G. Eckert. "Velocity Distributions, Temperature Distributions, Effectiveness and Heat Transfer for Air Injected Through a Tangential Slot into a Turbulent Boundary Layer," J. Heat Transfer, 83, 293-306 (1961b).

Hay, N., D. Lampard, and C.L. Saluja, "Effects of Cooling Fluids on the Heat Transfer Coefficient on a Flat Plate with Zero Mainstream Pressure Gradient," J. Engr. for Gas Turbine and Power, 107, 105-110 (1985a).

Hay, N., D. Lampard, and C.L. Saluja, "Effects of the Condition of the Approach Boundary Layer and of Mainstream Pressure Gradients on the Heat Transfer Coefficient on Film-Cooled Surfaces," J. Engr. for Gas Turbine and Power, 107, 99-104 (1985b).

Hiwada, M., K. Niwa, M. Kumada, and I. Mabuchi, "Effects of Tunnel Blockage on Local Mass Transfer from a Circular Cylinder in Cross Flow," Heat Transfer - Japanese Research, 8 (3), 37-51 (1979)

Jabbari, M.Y., and R.J. Goldstein. "Adiabatic Wall Temperature and Heat Transfer Downstream of Injection Through Two Rows of Holes," J. Engr. Power, 100, 303-307 (1978).

Karni, J., "Endwall Boundary Layer, Cylinder Diameter, Reynolds Number and Surface Injection Effects on Local Mass Transfer from a Cylinder in Crossflow," Ph.D. Thesis, University of Minnesota (1985).

Kear, B.H., "Advanced Metals," Scientific American, 255 (4), 158-167 (1986).

Kestin, J., and R.T. Wood. "The Influence of Turbulence on Mass Transfer from Cylinders," J. Heat Transfer, 93, 321-327 (1971).

Kumada, M., M. Hirata, and N. Kasagi. "Studies of Full-Coverage Film Cooling, Part 2: Measurement of Local Heat Transfer Coefficient," ASME Paper No. 81-GT-38 (1981).

Lander, R.D., R.W. Fish, and M. Suo. "External Heat Transfer Distribution on Film Cooled Turbine Vanes," J. Aircraft, 9(10), 707-714 (1972).

Liess, C. "Experimental Investigation of Film Cooling with Ejection From a Row of Holes for the Application to Gas Turbine Blades," J. Engr. Power, 97, 21-27 (1975).

Ligrani, P.M., and C. Camci. "Adiabatic Film Cooling Effectiveness from Heat Transfer Measurements in Compressible, Variable-Properties Flow," J. of Heat Transfer, 107, 313-320 (1985).

Ligrani, P.M., and F.A.E. Breugelmans. "Turbine Blade Cooling Research at the von Karman Institute for Fluid Dynamics." Paper presented at the Fifth International Symposium on Air Breathing Engines, Bangalore, India, February 1981.

Lowery, G.W., and R.I. Vachon. "The Effect of Turbulence on Heat Transfer from Heated Cylinders," Int. J. Heat Mass Transfer, 18, 1229-1242 (1975).

Luckey, D.W., D.K. Winstanley, G.J. Hanus, and M.R. L'Ecuyer. "Stagnation Region Gas Film Cooling for Turbine Blade Leading-Edge Applications," AIAA Journal of Aircraft, 14(5), 494-501 (1977).

Luckey, D.W., and M.R. L'Ecuyer. "Stagnation Region Gas Film Cooling - Spanwise Angled Injection From Multiple Rows of Holes," NASA CR-165333 (1981).

Mayle, R.E., and F.J. Camarata. "Multihole Cooling Film Effectiveness and Heat Transfer," J. Heat Transfer, 97, 534-538 (1975).

Metzger, D.E. "Developments in Air Cooling of Gas Turbine Vanes and Blades," ASME Paper No. 83-GT-160 (1983).

Metzger, D.E., H.J. Carper, and L.R. Swank. "Heat Transfer with Film Cooling Near Nontangential Injection Slots," J. Engr. Power, 90, 157-163 (1968).

Metzger, D.E., and D.D. Fletcher. "Evaluation of Heat Transfer for Film-Cooled Turbine Components," J.Aircraft, 8, 33-38 (1971).

Metzger, D.E., P.A. Kuenstler, and D.I. Takeuchi. "Heat Transfer with Film Cooling Within and Downstream of One to Four Rows of Normal Injection Holes No. 76-GT-83 (1976).

Mick, W.J., and R.E. Mayle. "Stagnation Film Cooling and Heat Transfer, Including Its Effect Within the Hole Pattern," J. of Turbomachinery, 110, 66-72 (1988).

Miller, K.L., and M.E. Crawford. "Numerical Simulation of Single, Double and Multiple Row Film Cooling Effectiveness and Heat Transfer," ASME Paper No. 84-GT-112 (1984).

Schmidt, E., and K. Wenner. "Warmeabgabe uber den Umfang eines angeblasenen geheizten Zylinders," Forschung, Geb. Ingwes, 12,(12), 65-73 (1941).

Sogin, H.H. "Sublimation from Disks to Air Streams Flowing Normal to Their Surfaces," Trans. ASME, 80, 61-71 (1958).

Sogin, H. and V.S. Subramanian, "Local Mass Transfer from Circular Cylinders in Cross Flow," J. Heat Transfer, 83, 483-493 (1961).